Many-body Green's function theory of ferromagnetic films with arbitrarily arranged single-ion anisotropies

Huai-Yu Wang,[1,2] S. U. Jen,[1] and Jing-Zhi Yu[2]
[1]*Institute of Physics, Academia Sinica, Nankang, Taiwan 11529*
[2]*Department of Physics, Tsinghua University, Beijing 100084, China*
(Received 23 September 2005; revised manuscript received 23 December 2005; published 15 March 2006)

In the treatment of Heisenberg Hamiltonian containing single-ion anisotropy by means of many-body Green's function method, the decoupling of the anisotropy term in higher order Green's functions usually takes an Anderson-Callen (AC) form. In this paper, possible improvement schemes of AC decoupling are discussed by comparison of the results with those of quantum Monte Carlo and frame rotation methods. We choose one scheme with a factor concerning the effect of the external field. Next, we discuss a possible difficulty of the frame rotation method in treating systems with single-ion anisotropies in more than one direction. Then we extended our method [Phys. Rev. B **70**, 134424 (2004)] to treat magnetic films. Some magnetic properties of ultrathin ferromagnetic films with thicknesses up to 16 monolayers are studied. The properties investigated include transition point, effective anisotropy coefficient, field-induced magnetization reorientation, and hysteresis loop. Several cases are investigated for uniaxial anisotropy and external field along different directions. The transition point, the effective anisotropy coefficient, the coercivity, and the loop area increase with increasing film thickness. The coercivity decreases and the loop area reduces with increasing temperature. The hysteresis loop along field direction is different from that along easy-axis direction. The coercivity and the area of the loop obtained in the former case are larger than the latter case. The reasons are analyzed by investigation of the trajectory of magnetization in detail. The influence of dipole interaction on the magnetic properties is discussed.

DOI: 10.1103/PhysRevB.73.094414 PACS number(s): 75.10.Jm, 75.70.Ak, 75.30.Gw

I. INTRODUCTION

Recently a technique has been developing to calculate magnetization with more than one component by use of the many-body Green's function method of quantum statistics under random phase approximation (RPA). Fröbrich *et al.*[1–3] first calculated the magnetization of ferromagnetic (FM) films by using three-component Green's function. We have applied the method to investigate antiferromagnetic films.[4] In these cases, the systems were magnetic films so that analytic expression was hard to obtain. However, in the cases of integer-dimensional FM systems, we have achieved a general analytic expression to calculate magnetization for any spin quantum number S, both for isotropic and anisotropic exchange cases.[5,6] The technique is a substantial extension of the old one by Tahir-Kheli *et al.*,[7–9] which dealt with only z-component magnetization when applied to treat various magnetic systems described by Heisenberg Hamiltonian.[10–14] The technique assumes that the three components of magnetization may all be nonzero. If two of them are zero, the results naturally go back to the z-component only case. Indeed, in this case our formula[5,6] naturally degrades to the form of that obtained by Callen *et al.*[7,8]

The key point of the technique is to construct three-order many-body Green's function matrix. Usually a set of spin operators S^+, S^-, and S^z is utilized, which makes use of convenient commutation between the operators. With this set of operators z axis is considered as a special direction and should be taken as the reference direction along which magnetization component should be nonzero. If there is a single-ion anisotropy in z direction, i.e., a term $-K_{2z}(S^z)^2$, appearing in Heisenberg Hamiltonian besides the exchange and Zeeman energy terms, the constructed Green's functions applies well.[1–6] However, when there are single-ion anisotropies in more than one direction, we found that it was more convenient to choose another set of spin operators S^x, S^y, and S^z.[15] This set of operators does not assume a special direction in space so that all the three spacial directions are equivalent. Therefore, one can easily take any direction as a reference direction as long as the magnetization component along this direction is not zero. We have achieved a general analytical expression to calculate magnetization for any spin quantum number S for integer-dimensional FM systems. We believed that similar to the way of Callen,[8] the expression of magnetization should be the solution of an ordinary differential equation (ODE). We indeed established such an ODE[16] and further found its solution.[17] The merit of the method makes it worth extending to magnetic films.

Henelius *et al.* calculated the magnetization of one monolayer (ML) ferromagnetic film by means of the quantum Monte Carlo (QMC) method.[18] Their results implied that the decoupling of higher order Green's function should be improved. Schwieger *et al.* used a frame rotation method (FRM) to calculate magnetization of one ML ferromagnetic film.[19] Their results agreed quite well with QMC. The merit of this method was that it did not need to construct a three-order matrix Green's function. However, they presented a simple case that single-ion anisotropy and external field were particularly arranged. For general arrangement geometry, there is probably one difficulty to overcome. By contrast, there is no difficulty for our method[15] to treat general geometry.

In Sec. II, we discuss the possible improvement of decoupling schemes. In Sec. III we discuss possible difficulty of FRM for general geometry. Section IV presents our numerical results of ferromagnetic films by means of our method.[15] The main concentration is put on hysteresis loops caused by anisotropies which is a topic not touched in the references cited above. The last section is the summary.

II. DISCUSSION OF IMPROVEMENT OF ANDERSON-CALLEN DECOUPLING

We first discuss a Heisenberg model with single-ion anisotropy in z direction and an external field.

$$H = -\tfrac{1}{2}J\sum_{(i,j)} \mathbf{S}_i \cdot \mathbf{S}_j - \sum_i K_{2z}(S_i^z)^2 - \sum_i \mathbf{B} \cdot \mathbf{S}_i. \tag{1}$$

In dealing with the model by many-body Green's function method, the decouplings of higher order Green's function are encountered. For exchange terms, Tyablicov decoupling, i.e., RPA, is used.[9] For single-ion term, there have been several decoupling scenarios. Devlin[20] compared these scenarios. According to his work, it seemed that Lines' decoupling[21] was a comparatively good approximation since it was valid in a wider range of anisotropy strength K_{2z}/J. This kind of decoupling scenario was employed in calculating only z component magnetization of ferromagnetic films.[12–14]

Recently, Fröblich *et al.*[2] thought that in calculating magnetization in more than one component, Lines' decoupling was not as good as the Anderson-Callen (AC) decoupling.[22] Since then, the AC decoupling has been mainly used.[23,6,15,16] One obvious advantage of the AC decoupling is that the expression is valid for all spin quantum number S. When K_{2z}/J is small, the results of the AC decoupling were almost identical to the exact ones.[20]

Henelius *et al.*[18] studied the effect of anisotropy strength on Curie point and reorientation of magnetization under external field along x direction by means of QMC and showed AC decoupling was valid only when both K_{2z}/J and the B_x/J were small. We here discuss possible improvements of AC decoupling by comparing the results with those of Refs. 18 and 19.

A. The effect of K_{2z}/J

The commutator of spin operator S^+ and the single-ion term in Hamiltonian Eq. (1) leads to a term $K_{2z}(S^+S^z+S^zS^+)$. The decoupling of this term usually takes the form of

$$K_{2z}(S^+S^z + S^zS^+) \rightarrow K_{2z}\Phi_z 2\langle S^z\rangle S^+. \tag{2}$$

The AC decoupling means that

$$\Phi_z = 1 - \frac{1}{2S^2}[S(S+1) - \langle S^zS^z\rangle]. \tag{3}$$

Let us consider the simplest case that magnetization points to z direction. When K_{2z}/J is small, this kind of decoupling does not bring any problem.[18,20] However, when K_{2z}/J became larger, the Curie point was overestimated.[18,20] That means that $K_{2z}\Phi_z$ should not be linearly proportional to K_{2z} but should increase less rapidly. We find that the following scheme can reduce the Curie point:

$$K_{2z}(S^+S^z + S^zS^+) \rightarrow \frac{J}{\gamma}\ln\left(1+\gamma\frac{K_{2z}}{J}\right)\Phi_z 2\langle S^z\rangle S^+. \tag{4}$$

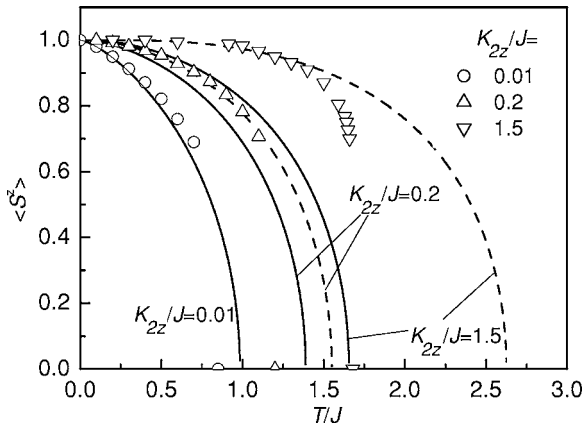

FIG. 1. Magnetization vs temperature curves of one ML FM film for different anisotropy strengths. Dashed lines are Eqs. (2) and (3) and solid lines are Eq. (4) with $\gamma=0.1$. Symbols are data of QMC (Ref. 18).

Figure 1 shows the results when $\gamma=0.1$ is taken. Unfortunately, the cost is that magnetization is underestimated below the Curie point. It is clear that when $\gamma K_{2z}/J \rightarrow 0$, Eq. (4) goes back to Eq. (2). In real materials K_{2z} is usually believed less than J in two order of magnitudes. In this paper, we only consider the case of small $K_{2z}/J=0.01$. Therefore, we do not use Eq. (4) in this paper.

B. The effect of external field B_x/J

Now we consider the case that the external field B_x is applied along the x direction perpendicular to the spontaneous magnetization. As B_x/J is small, QMC told us that the AC decoupling applied well. However, when B_x/J became larger, the behavior of magnetization reorientation was more like mean-field decoupling

$$K_{2z}(S^+S^z + S^zS^+) \rightarrow K_{2z}2\langle S^z\rangle S^+. \tag{5}$$

This is probably because when the spins turn to the field direction as the field increases, the spin fluctuation is more or less depressed. Therefore, we see that the factor Φ_z in Eq. (2) should depend on B_x/J. When B_x/J is small, Φ_z should be the form of Eq. (3), while as B_x/J goes larger, it should go to 1. The following form meets the conditions:

$$\Phi_z = 1 - e^{-\kappa B_x/K_{2z}}\frac{1}{2S^2}[S(S+1) - \langle S^zS^z\rangle]. \tag{6}$$

Figure 2 shows magnetization versus B_x/J curves of FM films with one and two MLs for spin quantum number $S=1$, 2, and 3 when $\kappa=0.25$. Since the calculation of FRM[19] well agreed with QMC, we regard FRM results as standard ones. Figure 2 also plots FRM results. For a two ML FM film, because the spin behavior in the two MLs are exactly the same, we obtain the analytic expressions of magnetization in

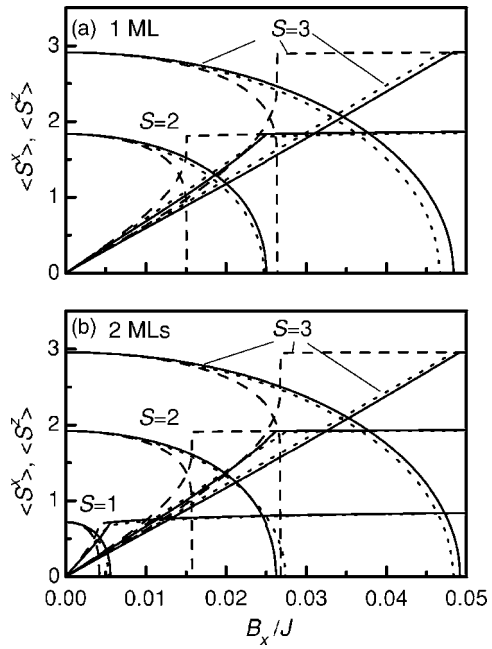

FIG. 2. Magnetization components of FM films with (a) one and (b) two MLs vs external field for spin quantum number $S=1$, 2, and 3 at temperature $T/J=1$. $\langle S^x\rangle$ starts from zero and increases while $\langle S^z\rangle$ decreases with B_x. Solid lines: Decoupling Eq. (6) with $\kappa=0.25$. Dashed lines: Decoupling Eq. (3). Dotted lines: FRM.

a way similar to one ML case for both our method[15] and FRM.[19] It is seen from Fig. 2 that Eq. (6) gives great improvement compared to Eq. (3).

The results of Fig. 2 are at temperature $T/J=1$. Figure 3(a) shows that the improvement depends on temperature. The magnetization reorientation is underestimated at a low temperature close to zero and overestimated at a high temperature close to Curie point. We find that a further temperature correction factor $(T/J)^\eta$, i.e.,

$$\Phi_z = 1 - e^{-\kappa B_x/K_{2z}}\left(\frac{T}{J}\right)^\eta \frac{1}{2S^2}[S(S+1) - \langle S^z S^z\rangle], \qquad (7)$$

can somehow improve the results. Figure 3(b) shows the results with $\eta=0.1$. Since the temperature correction factor does not give perfect correction, it is disregarded below.

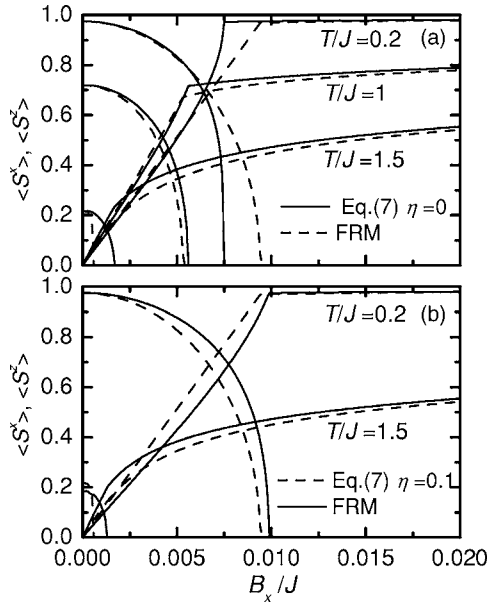

FIG. 3. Magnetization of a two ML FM film vs external field for $S=1$ at different temperature. $\langle S^x\rangle$ starts from zero and increases while $\langle S^z\rangle$ decreases with B_x. Solid line: Decoupling Eq. (5) with $\kappa=0.25$. Dashed lines: FRM. (a) $\eta=0$. (b) $\eta=0.1$.

In the following, the decoupling Eqs. (2) and (6) with $\kappa=0.25$ is used and the anisotropy strength is taken as two orders of magnitude less than Heisenberg exchange interaction. Under these conditions, we know from the discussion above that when the external field is absent or it is small, the magnetization versus temperature curve is right. When the temperature is in an intermediate region between zero and the Curie point, the magnetization versus field curves are right. When the temperature is close to zero or the Curie point, the magnetization versus field curves are not precise. Therefore, we mainly make comparisons between different arrangement geometry.

III. SINGLE-ION ANISOTROPIES IN MORE THAN ONE DIRECTION

In our previous paper,[15] we dealt with a more general case, that is, single-ion anisotropies were in more than one direction and the external field could be in any direction. The Hamiltonian is

$$H = -\tfrac{1}{2}J\sum_{(i,j)}\mathbf{S}_i\cdot\mathbf{S}_j - \sum_i [K_{2x}(S_i^x)^2 + K_{2y}(S_i^y)^2 + K_{2z}(S_i^z)^2] - \sum_i \mathbf{B}\cdot\mathbf{S}_i. \qquad (8)$$

It seems that this kind of system can also be studied by means of FRM.[19] In order to do so, one should first rotate the φ angle with respect to the z axis, then rotate the θ angle with respect to the resulting x axis, and finally rotate the ψ angle with respect to the resulting y axis. The rotation matrix should be

$$M = \begin{pmatrix} c_\theta c_\varphi & c_\theta s_\varphi & s_\theta \\ -s_\varphi c_\psi - s_\psi s_\theta c_\varphi & c_\psi c_\varphi - s_\psi s_\theta s_\varphi & s_\psi c_\theta \\ s_\varphi s_\psi - c_\psi s_\theta c_\varphi & -s_\psi c_\varphi - c_\psi s_\theta s_\varphi & c_\psi c_\theta \end{pmatrix}. \qquad (9)$$

Here we have shortened the triangle function as $c_\theta=\sin\theta$, $s_\theta=\sin\theta$, and so on. With the condition that in the new frame, the total spin operator $\Sigma_k S_k^{z\prime}$ should be a good quantum number: $[\Sigma_k S_k^{z\prime}, H]=0$, we get two equations:

$$(K_x s_\theta c_\theta s_\varphi + K_y c_\varphi c_\psi s_\theta s_\varphi s_\psi + K_z(c_\varphi s_\psi - s_\theta s_\varphi c_\psi)c_\theta c_\psi)C_1 + B_x c_\theta s_\varphi + B_y c_\varphi c_\psi + B_z(c_\varphi s_\psi - s_\theta s_\varphi c_\psi) = 0 \qquad (10)$$

and

$$(K_x s_\theta c_\theta c_\varphi + K_y c_\psi s_\theta s_\varphi^2 s_\psi + K_z(s_\varphi s_\psi - s_\theta c_\varphi c_\psi))c_\theta c_\psi C_1 + B_x c_\theta c_\varphi - B_y s_\varphi c_\psi + B_z(s_\varphi s_\psi - s_\theta c_\varphi c_\psi) = 0, \qquad (11)$$

where $C_1=\Phi_z 2\langle S^z\rangle$ with Φ_z being of the form of Eq. (3).

However, there are three angles φ, θ, and ψ to be determined. There should be one more condition. This difficulty is still to be overcome. Hence, in this paper, we still use the method suggested in Ref. 15.

IV. NUMERICAL RESULTS OF FM FILMS AND DISCUSSION

In this section, we calculate magnetization of FM films with L MLs. The Hamiltonian we deal with is as follows:

$$H = -\frac{1}{2}\sum_{\mu=1}^{L} J_\mu \sum_{(i,j)} \mathbf{S}_{\mu i}\cdot\mathbf{S}_{\mu j} - \sum_{\mu=1}^{L-1}\sum_{i} J_{\mu,\mu+1}\mathbf{S}_{\mu i}\cdot\mathbf{S}_{\mu+1,i}$$
$$- \sum_{\mu=1}^{L}\sum_{i}\left[K_{2x\mu}(S_{\mu i}^{x})^2 + K_{2y\mu}(S_{\mu i}^{y})^2 + K_{2z\mu}(S_{\mu i}^{z})^2\right]$$
$$+ \frac{g}{2}\sum_{\mu,\nu=1}^{L}\sum_{i,j}\frac{1}{r_{\mu i,\nu j}^{3}}\left[\mathbf{S}_{\mu i}\cdot\mathbf{S}_{\nu j} - (\mathbf{S}_{\mu i}\cdot\mathbf{u}_{\mu i,\nu j})(\mathbf{S}_{\nu j}\cdot\mathbf{u}_{\mu i,\nu j})\right]$$
$$- \sum_{\mu i}\mathbf{B}\cdot\mathbf{S}_{\mu i}. \tag{12}$$

The first term is the exchange interactions within each ML. The second term is the exchange energies between neighboring MLs. In these terms only the nearest neighbor exchanges are considered. The third term describes single-ion anisotropies in all three directions of space. The next term is the dipole interaction (DI) and the last term is the Zeeman energy arising from an external magnetic field. In Eq. (12) Greek letters μ and ν label monolayers, and i and j label sites in each ML. We let $\mathbf{r}_{\mu i,\nu j}$ denote the vector connecting sites μi (i site in μth ML) and νj (j site in νth ML). Then $\mathbf{u}_{\mu i,\nu j}=\mathbf{r}_{\mu i,\nu j}/r_{\mu i,\nu j}$ is the unit vector along this direction.

The method developed in our previous paper[15] is easily extended into the ferromagnetic film case. Here we only mention that for the on-site terms coming from the single-ion anisotropies a generalized form of the Anderson-Callen decoupling is used.[24]

$$\langle\langle S_{\mu i}^{\alpha}S_{\mu i}^{\beta} + S_{\mu i}^{\beta}S_{\mu i}^{\alpha}; B_{\nu j}\rangle\rangle = 2\langle S_{\mu i}^{\alpha}\rangle\Phi_{\mu\alpha}\langle\langle S_{\mu i}^{\beta}; B_{\nu j}\rangle\rangle + 2\langle S_{\mu i}^{\beta}\rangle\Phi_{\mu\beta}\langle\langle S_{\mu i}^{\alpha}; B_{\nu j}\rangle\rangle,$$
$$\alpha,\beta = x,y,z \quad \text{and} \quad \alpha\neq\beta, \tag{13}$$

where the factor $\Phi_{\mu\alpha}$ is assumed to have an identical form in all three spacial directions,

$$\Phi_{\mu\alpha} = 1 - e^{-\kappa B_{\alpha\perp}/J}\frac{1}{2S^2}[S(S+1) - \langle S_{\mu}^{\alpha}S_{\mu}^{\alpha}\rangle],\ \alpha = x,y,z. \tag{14}$$

Here $B_{\alpha\perp}$ is the field component perpendicular to axis α, e.g., $B_{x\perp}=\sqrt{B_y^2+B_z^2}$. The dipole interaction term is treated in the mean-field approximation as in Ref. 15.

For convenience in the following discussion, we name $\mathbf{M}_\mu=\langle\mathbf{S}_\mu\rangle$ as ML-magnetization and $\mathbf{M}=\frac{1}{L}\Sigma_{\mu=1}^{L}\langle\mathbf{S}_\mu\rangle$ as film-magnetization, or simply, magnetization.

Although the inter-ML exchanges can be either ferromagnetic or antiferromagnetic (AFM), in calculations below we consider FM exchanges only. The formulas derived enable us to study FM films with ML-dependent exchanges and anisotropies, but in this paper, we only study the cases of uniform exchange and anisotropy parameters. That is to say, $J_\mu=J_{\mu,\mu+1}=J$ and $(K_{2\mu x},K_{2\mu y},K_{2\mu z})=(K_{2x},K_{2y},K_{2z})$ for all MLs. The single-ion anisotropy strengths are set as $K_{2\alpha}/J=0.01$, $\alpha=x$, y, or z, and spin quantum number is taken as $S=1$. Usually, the DI strength g is two orders of magnitude smaller than the anisotropy parameter K_2. We take $g/J=0.000\,18$ in most cases as before.[2,15]

TABLE I. Five arrangements of single-ion anisotropy and field components studied in Sec. IV A.

Case	$(K_{2x}/J,K_{2y}/J,K_{2z}/J)$	$(B_x/J,B_y/J,B_z/J)$
A	(0.01,0,0)	0
B	(0,0,0.01)	0
A1	(0.01,0,0)	(0,0.002,0)
A2	(0.01,0,0)	(0,0,0.002)
B1	(0,0,0.01)	(0.002,0,0)

Since the case of one ML has been studied in the previous work,[15] here we investigate the cases of 2–16 MLs. In the following, we will investigate transition temperatures, the effective anisotropy coefficients, and magnetization reorientation angles in Sec. IV A, and hysteresis loops caused by uniaxial anisotropy in Sec. IV B.

A. Transition temperature, effective anisotropy coefficients and magnetization orientation angles

With the method developed in this paper, we are able to deal with various cases with the single-ion anisotropy and external field being arbitrarily arranged. For the sake of simplicity, we study in this subsection five arrangements listed in Table I. Cases A, A1, and A2 are of in-plane uniaxial anisotropy: In Case A there is no magnetic field applied; in Cases A1 and A2, a fixed field is applied in y and z directions, respectively. Cases B and B1 are of out-of-plane uniaxial anisotropy: In the former there is no magnetic field applied and in the latter a fixed field is applied in x direction. For Case B1 we can reproduce all the results obtained by Fröblich *et al.*, if using scaled parameters.[2]

We first calculate the magnetization. Since the field is fixed, the magnetization merely depends on temperature and film thickness. We do not show the magnetization versus temperature curves for each fixed film thickness because the curves are quite similar to those in Refs. 2 and 14.

Now let us discuss the transition temperatures at which the magnetization component along the easy axis becomes zero. For Cases A and B where there is no external field, the Curie temperatures are denoted as T_C(A) and T_C(B), respectively. For Cases A1, A2, and B1, each with a field perpendicular to the single-ion anisotropy direction, the magnetization gradually turns to the field direction with increasing temperature. The temperatures at which the magnetization just lie in the field direction are denoted by T_R(A1), T_R(A2), and T_R(B1), respectively. For convenience in the following

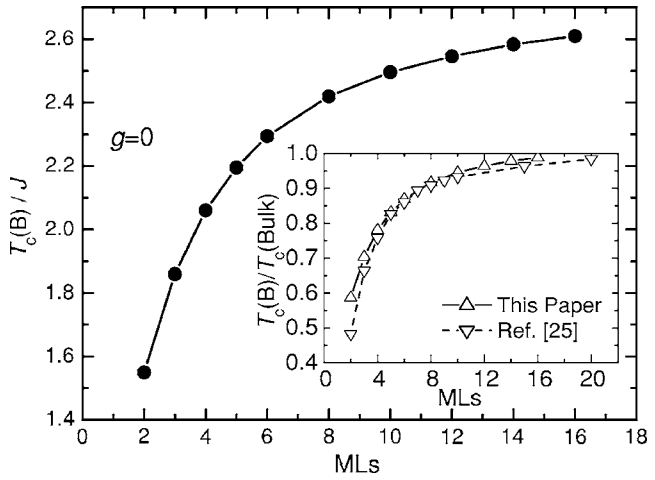

FIG. 4. Curie point $T_C(B)$ as a function of film thickness of Case B with $g=0$. Inset: Comparison with results of Ref. 25.

discussion, both T_C and T_R are regarded as transition temperature, or transition point.

T_C and T_R as functions of film thickness are obtained for all five cases. Figure 4 is the T_C-ML curve of Case B. The inset shows the comparison of our results with those of Ref. 25. The results are quite close to each other in disregard that the lattice here is simple cubic (sc) while there is face center cubic (fcc) lattice. The differences in 2 and 3 MLs seem large. We, however, notice that the experimental data between 2 and 3 MLs presented in Ref. 25 are larger than their results and closer to ours.

The T_C- and T_R-ML curves of all cases are close to each other. Here we give comparisons between different cases without presenting data. When $g/J=0.000\,18$, $T_C(\mathrm{A})-T_C(\mathrm{B})>T_R(\mathrm{A2})-T_C(\mathrm{B})>T_R(\mathrm{A1})-T_C(\mathrm{B})>0$ and $T_R(\mathrm{B1})-T_C(\mathrm{B})<0$, or $T_C(\mathrm{A})>T_R(\mathrm{A2})>T_R(\mathrm{A1})>T_C(\mathrm{B})>T_R(\mathrm{B1})$, some of which can be explained as follows.

DI plays a role of easy-plane anisotropy. It strengthens the in-plane anisotropy or weakens the out-of-plane uniaxial anisotropy, see Eq. (58) of Ref. 15. This is the key to understand the difference of transition temperatures of the five cases. Due to DI, the in-plane uniaxial anisotropy of Case A is stronger than the out-of-plane uniaxial anisotropy of Case B. A stronger uniaxial anisotropy leads to a higher T_C, thus $T_C(\mathrm{A})>T_C(\mathrm{B})$. For Cases A1 and A2, which are Case A plus a field along out-of-plane and within the film plane but perpendicular to the easy axis, respectively, the magnetizations turn to the field direction before the Curie point of Case A, so that $T_C(\mathrm{A})>T_R(\mathrm{A1})$ and $T_C(\mathrm{A})>T_R(\mathrm{A2})$. In Case A2, the magnetization turns from an in-plane direction to an out-of-plane direction, which is harder compared to Case A1 where magnetization turns within the film plane, because DI causes the in-plane anisotropy. Thus it is easily understood that $T_R(\mathrm{A2})>T_R(\mathrm{A1})$. For Case B1, which is Case B plus a field perpendicular to the out-of-plane direction, the magnetization turns from the easy-axis direction to the field direction before the Curie point of Case B, so that $T_C(\mathrm{B})>T_R(\mathrm{B1})$. In conclusion, $T_C(\mathrm{A})>T_C(\mathrm{B})>T_R(\mathrm{B1})$ and $T_C(\mathrm{A})>T_R(\mathrm{A2})>T_R(\mathrm{A1})$ when $g>0$.

As for why $T_R(\mathrm{A1})>T_C(\mathrm{B})$, we presently cannot give a convincing explanation.

To compare the transition point with and without DI, we also make numerical computations for $g=0$. When DI strength becomes zero, the easy-plane anisotropy will disappear. Therefore, there is no substantial difference between Cases A and B: $T_C(\mathrm{A})=T_C(\mathrm{B})$. For the same reason the numerical results of Cases A1, A2, and B1 should also become the same, i.e., $T_R(\mathrm{A1})=T_R(\mathrm{A2})=T_R(\mathrm{B1})$.

Now we compare the differences in transition points for each case with DI ($g/J=0.000\,18$) and without DI ($g=0$) to see the influence of DI strength. For Cases A, A1, and A2, the transition points with DI are higher than those without DI. The reason is that in all the three cases, the single-ion anisotropies are in the in-plane direction and the in-plane anisotropy is strengthened by DI, which results in the rise of transition points with the increase of DI strength g. While for Cases B and B1, the single-ion anisotropies are in the out-of-plane direction and weakened by DI. As a result, the transition points should become lower with the increase of DI strength g.

The effect of DI varies with film thickness. From Hamiltonian Eq. (12) one sees that the contribution of DI comes from both AFM and FM exchange interactions, the former is isotropic and the latter works along the line connecting two spins. In the case of one ML, the connecting lines are always in the film plane, so that DI results in a pure easy-plane anisotropy. For the films with more than one ML, as the lines connecting two spins in different MLs have a component projected to out-of-plane direction, the easy-plane anisotropy caused by DI should be comparatively weaker than that in one ML case. Therefore, the thicker the film, the comparatively weaker the easy-plane anisotropy caused by DI. That is to say, as film thickness increases, the effect of DI is weakened, or equivalently, the effect of the in-plane demagnetizing field is enhanced.

We also calculate the effective anisotropy coefficients and magnetization orientation angles for Cases A1, A2, and B1. If they are calculated by scaled parameters, their variations with temperature are quite similar to those in Refs. 2 and 15. Therefore, here we merely present their behavior with temperature and with MLs without giving numerical results.

As an example, let us see Case A1. The effective anisotropy coefficient $K_{2\mu x}(T)$ can vary with ML index μ. In the temperature region between zero and the transition point, the surface ML has the lowest value of $K_{2\mu x}(T)$ and the deeper the ML the larger the value. The reason is that $K_{2\mu x}(T)$ in each ML is closely related to the magnetization of this ML M_μ. The larger the M_μ, the larger the $K_{2\mu x}(T)$. The surface ML has the lowest magnetization and a deeper ML has a larger magnetization.[14,2,12] The effective coefficients at zero temperature are equal to the parameter in Hamiltonian, $K_{2\mu x}(0)=K_{2x}$. They decrease with increasing temperature, and become zero at and above transition point, $K_{2\mu x}(T\geqslant T_R)=0$. When the temperature is greater than zero, $K_{2\mu x}(T)$ increases with film thickness until transition point where it becomes zero.

Now we discuss the change of magnetization orientation angles with MLs and with temperature. At zero temperature, the magnetization orients near the easy axis, i.e., the angle between magnetization and easy axis is small (about 3 deg),

TABLE II. Six arrangements of single-ion anisotropy and varied field components studied in Sec. IV B.

Case	$(K_{2x}/J, K_{2y}/J, K_{2z}/J)$	$(B_x/J, B_y/J, B_z/J)$
C	(0.01,0,0)	(−0.03,0,0)−(0.03,0,0)
D	(0,0,0.01)	(0,0,−0.03)−(0,0,0.03)
C1	(0.01,0,0)	(−0.006,−0.02,0)−(0.006,0.02,0)
C2	(0.01,0,0)	(−0.006,0,−0.02)−(0.006,0,0.02)
C3	(0.01,0,0)	(−0.02,0,−0.01)−(0.02,0,0.01)
D1	(0,0,0.01)	(0,−0.02,−0.01)−(0,0.02,0.01)

because the field strength is much less than the single-ion anisotropy parameter. With the temperature increasing, the effective anisotropy coefficient decreases, so that the magnetization turns to the field direction. At the transition point, the coefficient becomes zero and the magnetization entirely lies in the field direction, so that the angle becomes 90 deg. In principle, the angles in different MLs can be different. However, calculated results show that the difference is negligible in each film thickness, indicating the fact that the ML-magnetizations are always parallel to each other because of FM exchange interaction. ML-magnetizations keep their initial angles until the temperature is very close to the transition point, and then quickly turn to the field direction just as in Refs. 2 and 15.

As we change DI strength g, the features of effective anisotropy coefficients and reorientation angles remain qualitatively unchanged. The discussion is similar to that in Ref. 15. In the present calculation the field $B/J=0.002$ is not strong. The effect of field strength on a one-ML FM film was discussed in Refs. 1 and 15. The discussion of the multi-ML FM film is similar so that it is not presented here.

B. Hysteresis loops

One can apply a varied magnetic field in a fixed direction to investigate the magnetization versus field curve of an ultrathin magnetic film. The curves for the increasing and decreasing fields are different due to the uniaxial anisotropy of the film, which results in hysteresis loops. In this subsection, we study six cases listed in Table II.

Cases C, C1, C2, and C3 are Case A with a field in different directions: In Case C the field is in x direction, the single-ion anisotropy direction; in Case C1 the field is in the xy plane; in Cases C2 and C3, the field is in the xz plane, where the field direction is closer to x direction in the latter than in the former. In these four cases, the x direction is the uniaxial direction. Cases D and D1 are Case B with a field applied in different directions: In Case D the field is in the z direction, while in the latter the field is in the yz plane. In these two cases, the z direction is the uniaxial direction. In each case, the field varies linearly in the fixed direction.

Figure 5 shows the hysteresis loops of Cases C and D. We first discuss the results of Case C. In this case the field is applied along the x axis, the uniaxial direction. Let us discuss the magnetizing procedure when the field varies from negative to positive. If there is a strong field applied in the negative x direction, the magnetization is parallel to the field direction. When the field is weakened gradually, the magnetization also decreases slightly. As the field goes to zero and even just reverses, the magnetization still keeps its orientation unchanged so that it becomes antiparallel to the positive field, as the Zeeman energy has not yet been large enough to overwhelm the anisotropy energy. When the positive field is sufficiently strong, the magnetization will be forced to reverse so as to turn to the direction parallel to the field. In the same way one can discuss the magnetizing procedure when the field varies from positive to negative. The magnetization curves with increasing and decreasing fields consist of hysteresis loop, which is depicted by solid lines in Fig. 5.

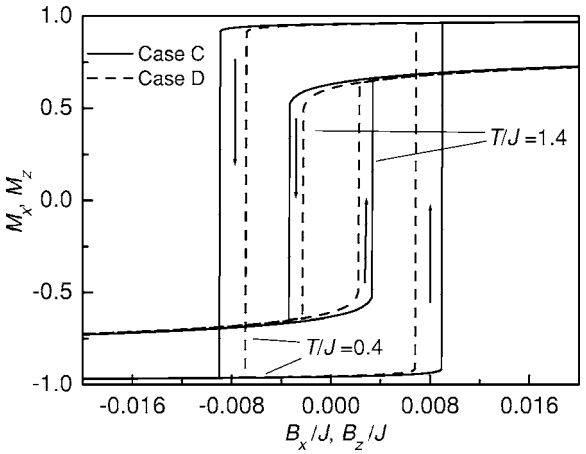

FIG. 5. Hysteristic loops of a three ML FM film. Solid lines: Case C. The x axis is B_x and y axis is M_x. Dashed lines: Case D. The x axis is B_z and y axis is M_z. The outer loops are for lower temperature $T/J=0.4$ and the inner loops are for higher temperature $T/J=1.4$.

For Case D, the discussion is similar. In this case the field is applied along the z axis, the uniaxial direction. The produced loop is depicted by dashed lines in Fig. 5.

Now let us compare the results of Cases C and D. Obviously, the larger the uniaxial anisotropy, the larger the coercivity and the loop area. For Cases C and D, the single-ion anisotropy strengths are the same, but their coercivities are different, see the solid and the dashed lines in Fig. 5. This difference comes from DI. Because DI acts as an additional easy-plane anisotropy, the effective anisotropy coefficient of Case C is larger than that in Case D. As a result, the coercivity of a solid-line loop is larger than that of a dashed-line loop. The smaller the DI strength, the closer the solid and dashed lines will be. If DI disappears, the loops generated in the case of in-plane uniaxial anisotropy and out-of-plane uniaxial anisotropy will be the same, and the solid and dashed lines in Fig. 5 will become identical.

Figure 5 also shows the influence of temperature on the hysteresis loops. At $T/J=0.4$, the loops manifest almost rectangular shape. While at $T/J=1.4$, the loops become narrower and deviate from rectangular shape. The change is caused by two factors. One is that the magnetization is nearly saturated at a low temperature close to zero, and it decreases with increasing temperature. The other is that the effective aniso-

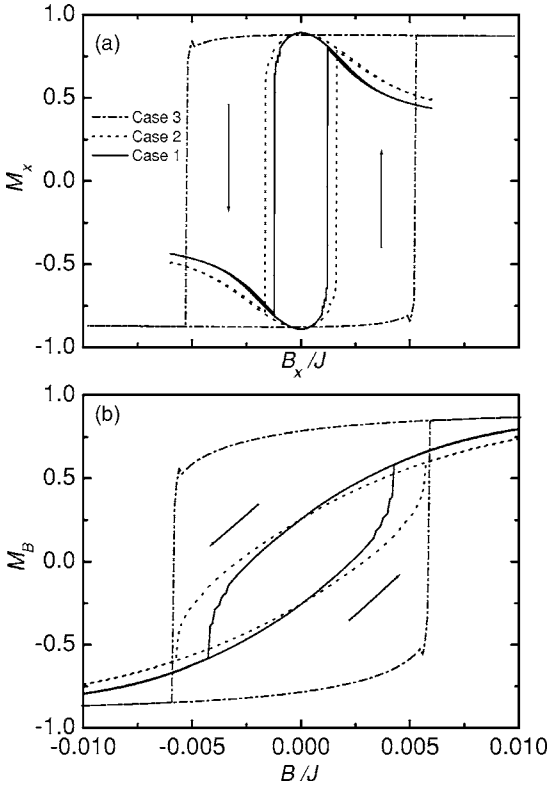

FIG. 6. Hysteristic loops along different directions of a three ML FM film for Case C1 (solid lines), Case C2 (dotted lines), and Case C3 (dash-dotted lines) at temperature $T/J=0.8$. (a) M_x vs B_x/J. (b) Magnetization projected to direction of the field, M_B, vs field B/J.

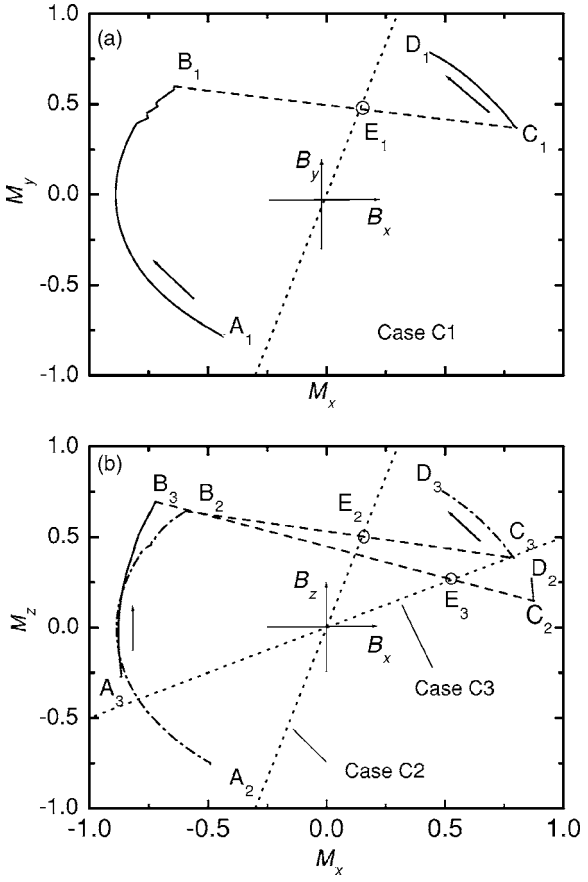

FIG. 7. The trajectories of magnetization vectors of a three ML FM film for Cases C1, C2, and C3 with increasing field at $T/J=0.8$. Dotted lines show the field directions. (a) For Case C1, the magnetization moves from A_1 to B_1, then leaps to C_1 and goes to D_1. (b) For Case C2, the magnetization moves from A_2 to B_2, then leaps to C_2 and goes to D_2. For Case C3, the magnetization moves from A_3 to B_3, then leaps to C_3 and goes to D_3. In both panels, the dashed lines merely show the leaps. The crosspoints of dashed and dotted lines, E_1, E_2, and E_3, demonstrate the B/J values at which the magnetizations reverse.

tropy coefficient lowers as the temperature rises. These two factors lead to smaller coercivity and magnetization at a higher temperature. Figure 5 shows that the difference of the coercivity between Cases C and D becomes smaller as the temperature rises. The coercivities of solid and dashed loops are 0.008 95 and 0.006 85 at $T/J=0.4$, and are 0.003 35 and 0.002 25 at $T/J=1.4$.

The above results are for the cases in which the field is applied to the direction of easy axis. In the following, we investigate the cases where the field is applied along a direction other than the easy axis.

Figures 6 and 7 are the results of Cases C1, C2, and C3. Figure 6(a) depicts the M_x–B_x curves, which compose hysteresis loops. Figure 6(b) depicts the hysteresis loops composed by M_B–B curves when the magnetization component along the field direction is taken. Figure 7 shows the trajectories of magnetization vectors with increasing fields.

We first discuss Case C1. Since the field is applied in the xy plane and the magnetization has two components M_x and M_y, the magnetizing procedure with the field varying from negative to positive is as follows. As there is no single-ion anisotropy along the y direction, y component of magnetization M_y decreases with weakened B_y. When **B** goes to zero, M_y also becomes zero. However, because the easy axis is in the x direction, x component of magnetization M_x does not approach zero even when B_x becomes zero. The M_x–B_x curve is depicted by the solid line in Fig. 6(a).

Magnetization orients between the field direction and the easy-axis direction, and it is closer to the field direction for stronger field and closer to easy axis for weaker field. That is to say, M_x becomes larger as the field decreases. When $\mathbf{B}=0$, the magnetization turns to x axis and there is no y component M_y, so that M_x reaches its maximum, see the solid lines in Fig. 6(a). When the field reverses from a positive to negative direction, negative M_y appears, which means that the magnetization deviates from x axis. However, the x-component M_x remains its orientation unchanged when B_x is small. As the negative B_x is strong enough, M_x is forced to reverse. The analysis is the same for the magnetizing procedure with the field varying from positive to negative. As a result, M_x curves show a loop. The feature of the loop is that the value of M_x within the loop area is larger than that in the tail areas. The smaller the B_x component of the field, the smaller M_x will be in tail areas. Nevertheless, the value of M_x at $B_x=0$ remains unchanged.

Jen *et al.*[26,27] have studied the experimental M_x-hysteresis and M_y-hysteresis loops in Case C1 in detail by employing

vector vibrating sample magnetometer. The calculated results here agree with the experiments. For example, the theoretical plot of the M_x-hysteresis here in Fig. 6(a) is the same as the experimental plot of the M_y-hysteresis in Fig. 2(d) of Ref. 26 or Fig. 3(b) of Ref. 27. Figure 9(b) of Ref. 28 gave an experimental example that the field was entirely transversal, i.e., perpendicular to the measured magnetization component.

Experimentally, the magnetization is also often measured along the field. Therefore, we plot the curves of magnetization projected to the field direction by solid lines in Fig. 6(b). The curves also compose hysteresis loop. Comparing the loop with that in Fig. 6(a), we see two remarkable distinctions. One is that the coercivities in Fig. 6(b) are greater than that in Fig. 6(a). The other is that in Fig. 6(b) the values of M_B in the loop area are less than those in tail areas, while in Fig. 6(a) the value of M_x within the loop area can be greater than that in tail areas as mentioned above. In order to explain these two distinctions, we investigate the trajectory of magnetization vector.

The solid lines in Fig. 7(a) present the trajectory of the magnetization vector as the field increases from negative to positive. As the field is in the third quadrant and strong enough, the magnetization is also in this quadrant, and its direction is between the field direction and x axis which is the easy axis. As the field is weakened, the magnetization gradually turns to easy axis. As $\mathbf{B}=0$, it lies in the x axis, and the component M_x becomes maximum. As $\mathbf{B}$ increases in the first quadrant, there appears a positive M_y component so that the magnetization deviates from the x axis and enters the second quadrant. When positive B_x becomes large enough, M_x is forced to reverse so that the magnetization leaps to the first quadrant and its direction is again between the field and x axis. After that, with the increasing field, the magnetization turns to the field direction. In a word, the trajectory of the magnetization starts from A_1 and goes to B_1, and then leaps to C_1 and continues going to D_1. In Fig. 7(a), the dashed line connecting points B_1 and C_1 merely demonstrates the leap. The crosspoint of the dashed and dotted lines, point E_1, is just the field at which magnetization reverses.

In Fig. 7(a), when one projects the magnetization to the x axis, he obtains M_x. The M_x–B_x curves compose the loop in Fig. 6(a). When he projects magnetization to the field direction, he obtains M_B. The M_B–B curves compose the loop in Fig. 6(b). Now we can explain the two distinctions between the solid loops in Figs. 6(a) and 6(b). At crosspoint E_1, the value of the field B is larger than its projection in B_x axis. The former is the value of the coercivity of the solid loop in Fig. 6(b) and the latter is the coercivity of the solid loop of that in Fig. 6(a). Therefore, the coercivities in Fig. 6(b) are greater than that in Fig. 6(a). In Fig. 7(a), when the magnetization vector moves from A_1 point to B_1 point, its projection to the dashed line direction, M_B, gradually decreases, while its projection to x axis, M_x, first increases and reaches the maximum when it lies in the x axis, and then gradually decreases. That is why in Fig. 6(b), M_B within the loop area is smaller than in tail areas, while in Fig. 6(a) M_x within the loop area can be larger than in tail areas.

Here we should point out that the loop area in Fig. 6(a) is smaller than that in Fig. 6(b). The reason is that the former means the work done by only the x-component of the field, B_x, while the latter means the work done by the field $B=\sqrt{B_x^2+B_y^2}$.

For Case C2, the discussion is similar. In this case the field is applied in xz plane and the magnetization has two components M_x and M_z. The dotted lines in Fig. 6(a) show the loop of M_x–B_x and those in Fig. 6(b) show the loop of M_B–B. The trajectory of the magnetization vector with increasing field is plotted as dash-dotted lines in Fig. 7(b). It starts from A_2 and goes to B_2, and then leaps to C_2 and ends at D_2.

In Cases C1 and C2, the field components along the easy axis are the same, but the coercivities of the M_x–B_x loops are not the same, as can be seen by comparison of solid and dotted loops in Fig. 6(a). The difference again comes from DI. In Case C1 where the field has two components B_x and B_y, DI affects as if there is an additional and equivalent field along both x and y directions, see Eq. (59) of Ref. 15. While in Case C2 where the field has two components B_x and B_z, the effect of DI is to strengthen B_x and to weaken B_z, again see Eq. (59) of Ref. 15. Comparatively, the integrated B_x ingredient is slightly smaller in Case C1 than in Case C2. That results in a smaller coercivity of the M_x–B_x loop of the former than that of the latter.

The M_x–B_x loop and M_B–B loop of Case C3 are plotted in Figs. 6(a) and 6(b), respectively, both by dash-dotted lines. In this case, the field is again in xz plane, but is closer to the easy axis, i.e., B_x component is comparatively larger than Case C2. Therefore, the coercivity is greater than Case C2, as can be seen by comparison of the dash-dotted loop and the dotted loop in Fig. 6(a). The trajectory of the magnetization vector with an increasing field is shown in Fig. 7(b) by solid lines. It starts from A_3 and goes to B_3, and then leaps to C_3 and ends at D_3.

In Fig. 7(b), the x component of the field at the leap point E_3 is larger than that of leap point E_2. Hence, the closer the field direction to the x axis, the larger the coercivity of the M_x–B_x loop will be. If the field entirely lies down to the x axis, Case C3 will become Case C and the hysteresis loop will become the solid line in Fig. 5.

In Fig. 7, the trajectory curves are all with increasing field. The trajectories with decreasing field are all symmetric to the curves in Fig. 7 with respect to origin.

Finally, let us see the out-of-plane uniaxial anisotropy case, Case D1. The field is applied in the yz plane and the magnetization has two components M_y and M_z. Please note that in this case z axis is the easy axis. Figures 8(a) and 8(b) show the M_z–B_z loop and M_B–B loop, respectively. The trajectory of the magnetization vector with increasing field is plotted in Fig. 9. The analysis is quite similar to that for Case C1, so it is not presented here.

In Figs. 8 and 9 also shown is the effect of temperature. The solid lines are the results at $T/J=0.5$ and the dash-dotted lines are those at $T/J=1.5$. At a higher temperature, the coercivity and loop area are smaller than those at a lower temperature, a feature which is the same as in Fig. 5. At a lower temperature, the magnetization is closer to the saturated value. So we mainly see the magnetization rotation besides the leap, see the solid lines in Fig. 9. While at a higher temperature, the magnetization is far from saturated. As the

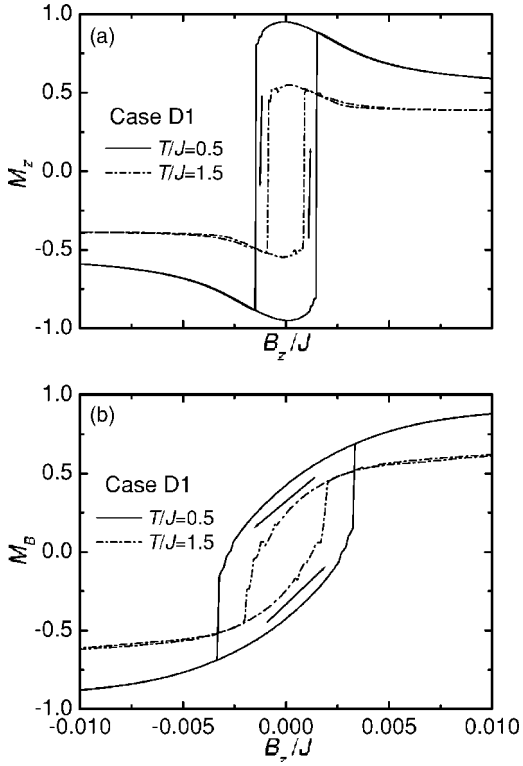

FIG. 8. Hysteristic loops for a 3 ML FM film for Case D1 at temperatures $T/J=0.5$ (solid lines) and $T/J=1.5$ (dash-dotted lines). (a) M_z vs B_z/J. (b) Magnetization projected to direction of the field, M_B, vs field B/J.

field becomes stronger, the magnetization will increase, see Fig. 8(b) and the regions near points A_2 and D_2 in the dash-dotted lines in Fig. 9, as well as the approach to the field direction.

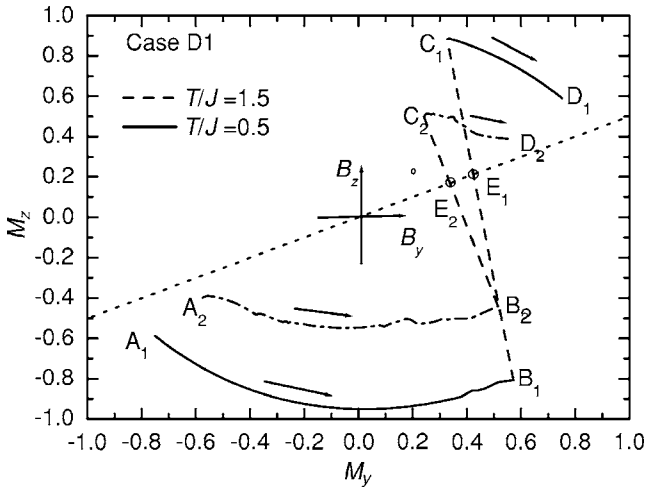

FIG. 9. The trajectory of magnetization vector of a 3 ML FM film for Case D1 with increasing field at temperature $T/J=0.5$ (solid lines) and 1.5 (dash-dotted lines). The dotted lines show the field directions. The dashed lines merely show the leaps. The cross-points of dashed and dotted lines, E_1 and E_2, demonstrate the B/J values at which the magnetizations reverse.

V. SUMMARY

In this paper, firstly, we discuss possible improvement schemes of the AC decoupling by comparing the results with those of QMC and FRM, and choose one scheme with a factor concerning the effect of the external field, neglecting those concerning the effects of anisotropy strength and temperature. Secondly, we discuss a possible difficulty in using FRM to treat the system with magnetization in an arbitrary direction.

Then the method in Ref. 15 dealing with magnetic systems with single-ion anisotropies in more than one direction is extended to treat films. The method turns out its availability in studying ultrathin FM films. For several cases with the anisotropy and external field in different directions, we investigate magnetic properties including transition point, effective anisotropy coefficient, field-induced magnetization reorientation, and hysteresis loop, and their dependence on temperature and film thickness. The effect of DI is also discussed.

In all the cases, the transition point increases with film thickness. In the cases that there is DI, the magnetization is easier to turn from out-of-plane to in-plane direction, or more difficult to turn in a contrast way, compared to the cases without DI. The effects of DI can always be considered as an effective in-plane anisotropy or an in-plane field as has been analyzed in Ref. 15. However, this effect abates with film thickness increasing.

The effective anisotropy coefficient $K_2(T)$ decreases with increasing temperature. If calculated in scaled parameters, it equals to the parameter in the Hamiltonian at zero temperature, and becomes zero when the temperature reaches the transition point. For a given film the value of the effective anisotropy coefficient is different from ML to ML in the temperature range between 0 K and transition point. The surface ML has the lowest value and the deeper the ML, the larger the value. Nevertheless, the difference is trivial for the third and the deeper MLs.

The magnetizations of all MLs in one FM film rotate uniformly subject to a fixed external field. That is to say the azimuth angles of them are almost identical to each other at any temperature. Under a comparatively weak field, $B/K_2=0.2$, the azimuth angle of the magnetization of the film remains at its initial angle, the angle at zero temperature, almost unchanged within a wide temperature range. Close to the transition point, the magnetization quickly turns to the field direction.

The uniaxial anisotropy of a FM film can generate hysteresis loop. At a lower temperature the coercivity and the loop area are larger than those at a higher temperature. This is because both the magnetization and the effective anisotropy coefficient at a lower temperature are larger than those at a higher temperature. The DI acts as an additional easy-plane anisotropy. Therefore, when the field direction is in the film plane, the coercivity and loop area with DI are larger than those without DI.

The external field may be applied in a direction other than easy axis. The calculation shows that if the loops are measured along the field direction, the magnetization in the loop area is lower than in tail areas. However, if the loops are

measured along the easy-axis direction, the magnetization in the loop area is higher than that in tail area. The trajectory of the magnetization clearly shows its behavior under an external field.

[1] P. Fröbrich, P. J. Jensen, and P. J. Kuntz, Eur. Phys. J. B **13**, 477 (2000).

[2] P. Fröbrich, P. J. Jensen, P. J. Kuntz, and A. Ecker, Eur. Phys. J. B **18**, 579 (2000).

[3] P. Fröbrich, P. J. Kuntz, and M. Saber, Ann. Phys. **11**(5), 387 (2002).

[4] Huai-Yu Wang, Chen Huang, Meichun Qian, and En-Ge Wang, J. Appl. Phys. **95**, 7551 (2004).

[5] Huai-Yu Wang, Ke-Qiu Chen, and En-Ge Wang, Int. J. Mod. Phys. B **16**(25), 3803 (2002).

[6] Huai-Yu Wang, Chong-Yu Wang, and En-Ge Wang, Phys. Rev. B **69**, 174431 (2004).

[7] R. A. Tahir-Kheli and D. Ter Haar, Phys. Rev. **127**, 88 (1962).

[8] H. B. Callen, Phys. Rev. **130**, 890 (1963).

[9] S. V. Tyablikov, *Methods in the Quantum Theory of Magnetism* (Plenum, New York, 1967).

[10] Huai-Yu Wang, Ke-Qiu Chen, and En-Ge Wang, Phys. Rev. B **66**, 092405 (2002).

[11] Huai-Yu Wang, Shan-Ying Wang, Chong-Yu Wang, Wen-Hui Duan, and Ke-Qiu Chen, J. Phys.: Condens. Matter **15**, 2783 (2003).

[12] Huai-Yu Wang, Yun-Song Zhou, Chong-Yu Wang, and D. L. Lin, Chin. Phys. **11**(2), 167 (2002).

[13] W. Guo, L. P. Shi, and D. L. Lin, Phys. Rev. B **62**, 14259 (2000).

[14] R. Schiller and W. Nolting, Solid State Commun. **110**, 121 (1999).

[15] Huai-Yu Wang, Zhen-Hong Dai, P. Fröbrich, P. J. Jensen, and P. J. Kuntz, Phys. Rev. B **70**, 134424 (2004).

[16] Huai-Yu Wang, Bin Zhou, and Nian-Xian Chen, Commun. Theor. Phys. **43**, 753 (2005).

[17] Huai-Yu Wang, Yao Long, and Nian-Xian Chen, Commun. Theor. Phys. **45**, 175 (2006).

[18] P. Henelius, P. Fröbrich, P. J. Kuntz, C. Timm, and P. J. Jensen, Phys. Rev. B **66**, 094407 (2002).

[19] S. Schwieger, J. Kienert, and W. Nolting, Phys. Rev. B **71**, 024428 (2005).

[20] J. F. Devlin, Phys. Rev. B **4**, 136 (1971).

[21] M. E. Lines, Phys. Rev. **156**, 534 (1967).

[22] F. B. Anderson and H. B. Callen, Phys. Rev. **136**, A1068 (1964).

[23] P. Fröbrich and P. J. Kuntz, Phys. Rev. B **68**, 014410 (2003).

[24] In Ref. 15, the plus sign on the right hand side of Eq. (11) was misprinted as an equal sign.

[25] W. Müller and W. Nolting, Phys. Rev. B **69**, 155425 (2004).

[26] S. U. Jen and W. L. Chen, J. Appl. Phys. **87**, 8640 (2000).

[27] S. U. Jen and J. Y. Lee, J. Magn. Magn. Mater. **271**, 237 (2004).

[28] J. Prokop, D. A. Valdaitsev, A. Kukunin, M. Pratzer, G. Schönhense, and H. J. Elmers, Phys. Rev. B **70**, 184423 (2004).